大韓土木學會論文集
第13卷 第1號 · 1993年 3月
pp. 193~201

심해파의 불안정성에 관한 실험 연구

제 1 부 : 정상파의 불안정성

Experimental Study of Deep-Water Wave Instability : Part 1. Evolution of The Uniform Wave Train

조 원 철*
Cho, Won Chul

Abstract

Experimental investigation of nonlinear instability of deep-water wave train is performed. Two-dimensional Benjamin-Feir type wave instability and breaking are observed at wave steepness between 0.19 and 0.25 and three-dimensional instability and breaking at wave steepness greater than or equal to 0.31. At the same wave steepness, shorter waves with smaller amplitude are more unstable, with earlier occurrence of breaking, than long waves with large amplitude.

요 지

심해 정상파의 불안정성에 관한 실험 연구로부터, 파형경사 0.19에서 0.25 사이에서는 2차원적인 Benjamin-Feir 형태의 불안정성과 쇄파가 관찰되었으며, 파형경사가 이보다 큰 0.31 이상에서는 3차원적인 불안정성과 쇄파가 관찰되었다. 또한 이 실험에서 같은 파형 경사를 가진 2가지 종류의 파랑이 실험, 관찰되었는데, 여기에서 작은 파고를 가진 짧은 파랑은 높은 파고를 가진 긴 파랑보다 더 불안정하고 그리고 보다 더 빨리 쇄파됨이 관찰되었다.

1. Introduction

During the past two decades, many studies have been carried out to understand the evolution of nonlinear deep-water wave train. In 1967, Benjamin and Feir discovered that a steep uniform deep-water wave train with constant wave frequency becomes highly irregular and unstable and finally breaks far from its origin due to infinitesimal perturbations in a pair of side-band frequency components. Longuet-Higgins (1978) investigated perturbations of steep deep-water gravity waves with arbitrary wave steepnesses. He found that as the wave steepness was increased, the perturbation became unstable and followed the Benjamin-Feir instability until the wave steepness reached 0.346 (called subharmonic instability, in which perturbation of the horizontal scale is greater than the basic wavelength). The maximum growth rate was observed at wave steepness, $ka=0.32$ (k is wavenumber and a is wave amplitude). However, beyond that region the stability was established again and at about $ka=0.406$, a new and

* 정회원 · 중앙대학교 기술과학연구소 선임연구원

very strong instability appeared with a much higher rate of growth, similar to the superharmonic instability (which has a perturbation of the horizontal scale equal to or less than the basic wavelength). McLean (1982) carried out a numerical investigation on the stability of a finite amplitude wave train in deep water to infinitesimal three-dimensional disturbances. He demonstrated that there were two types of instabilities, Class I and Class II ; Class I was a two-dimensional instability that occurred in the range of wave steepness less than 0.31, which corresponds to the Benjamin-Feir instability. Class II was the fully three-dimensional instability, which developed fast and became much stronger than the Class I instability, in the range between ka=0.31 and ka=0.41.

Melville (1982) studied uniform deep-water wave instability and breaking, and confirmed two-dimensional Benjamin-Feir instability as well as three-dimensional instability. It was also found that at the initial stage of the wave evolution, the upper and the lower side-band frequencies were developed asymmetrically about the fundamental frequency and its higher harmonics (the upper side-band frequency being larger than the lower side-band frequency). However, at the onset of breaking, the lower side-band frequency grew rapidly and became dominant in the wave field after breaking. Su et. al. (1982) performed an experimental work and also observed two-dimensional and three-dimensional instabilities and large growth of the lower side-band frequency after breaking, showing frequency downshift as much as 25 % of the fundamental wave frequency.

Most laboratory studies on the nonlinear instability of deep-water wave train have been based on Benjamin and Feir's wave instability. In the present study, uniform deep-water wave instability and breaking are investigated not only by constant wave frequency with various wave amplitudes but also by constant wave amplitude with various wave frequencies.

2. Theory

A theoretical analysis of wave instability was presented by Benjamin and Feir (1967), who showed that a periodic progressive wave train with fundamental frequency, ω, and finite amplitude in deep water is unstable to small perturbations in the form of a pair of side-band frequency components, $\omega(1\pm\delta)$, where d is a small perturbation in the wave frequency of the order (ka). They studied the stability of a Stokes wave train on a two-dimensional irrotational, inviscid and incompressible fluid in infinitely deep water by means of a linearlized perturbation analysis. They found in their analysis that a uniform continuous wave train is unstable to infinitesimal perturbations in side-band frequencies when is in the range between 0 and $\sqrt{2}$ ka. They derived Eqn(2.1.2) for the perturbed free-surface elevation, $\eta(x,t)+\varepsilon(x,t)$, which is corresponding to a nearly uniform wave train with a weak amplitude modulation, from the surface elevation, Eqn(2.1.1), which includes the first two harmonics.

$$\eta(x,t)=a\ \cos(kx-\omega t)+1/2ka^2\cos2(kx-\omega t) \tag{2.1.1}$$

$$\eta_p(x,t)=a\ \cos(kx-\omega t)+\varepsilon_+\cos[k(1+\kappa)x-\omega(1+\delta)t]+\varepsilon_-\cos[k(1-\kappa)x-\omega(1-\delta)t] \tag{2.1.2}$$

where κ and δ are small perturbations in the wavenumber and frequency respectively. $\varepsilon_{\pm}=\exp[1/2\delta\ (2k^2a^2-\delta_2)^{1/2}\omega t]$ represents the amplitude of the side-band disturbances. $\eta_p(x,t)$ displays a gradual modulation of the fundamental waveform, a $\cos(kx-\omega t)$. For a given value of the wave steepness, ka, of the initial wave, the unstable side-band amplitude grow exponentially with time if $0<\delta\leq\sqrt{2}ka$, with the growth rate having a maximum value at $\delta=ka$.

When these results are applied to an experimental work, in which a nearly uniform and weakly nonlinear wave is generated from a wavemaker at one end of a wave tank(at x=0) and deveolps with distance, we need only to replace t by $C_g=2kx/\omega$. Therefore, the spatial growth of side-band modes generated with fixed frequencies $\omega(1\pm\delta)$ at x=0 are

$$\varepsilon_{\pm}\cong\exp[\delta(2k^2a^2-\delta^2)^{1/2}kx] \tag{2.1.3}$$

The condition of instability is still the same as before, $0<\delta\leq\sqrt{2}ka$.

3. Experiment

3.1 Experimental Apparatus

Experiments were performed at Davidson Laboratory of Stevens Institute of Technology in Hoboken, New Jersey, U.S.A., where the wave channel is 313 feet long, 12 feet wide, and the water depth is 5.4 feet. The fresh water is filled in the wave channel and continuously filtered. The side walls of the wave channel are concrete, with no opening to observe the water column outside the tank.

The wave channel is equipped with dual-flap hydraulic wavemaker at one end and a wave absorbing beach at the other. The dual flap is composed of lower flap and upper flap in which the lower flap is hinged on the channel floor and the upper flap is hinged on the top of the lower flap. The wavemaker is controlled by PDP-11 microcomputer which calculates the digital signal form of the flap motion as a function of time from a given wave frequency and height. These digital time series are converted to control voltage corresponding to the stored digital sequence at a predetermined time interval through the digital-to-analog converter. Then, the hydraulic servo system produces a sepecific wave form proportional to the applied sinusoidal flap angles. Since, the wavemaker control is accomplished by programming the microcomputer, appropriate computer programming allows one to generate regular waves, random waves, and virtually any type of wave form.

The wooden sloping beach at one end dissipates propagating wave and absorbes incident wave energy to minimize wave reflection during tests. Owing to the relatively long wave channel, the waves were not disturbed by wave reflection from the beach, which may yield slow modulations to the incident waves. To avoid any possible effect of wave energy reflection, measurements were completed within 4 minutes before wave energy was reflected to the measuring station. Data collection was begun after the first wave arrived at the beach and a proper steady state of wave evolution was achieved. All tests were started after calm water was obtained, with the time to calm water between runs taken about 30 minutes.

Evolution of the surface wave train was measured as waves propagated down the channel, using 5 wave gauges located at 20, 70, 120, 170, and 220 feet downstream from the wavemaker. Three wave gauges were also installed cross the wave channel, spaced 1 foot apart from one side wall and 70 feet downstream from the wavemaker, to measure the transverse perturbations along the wave crest which cause the wave train to evolve to a three-dimensional wave instability at large wave steepness. Wave gauges were calibrated before every daily measurement using vertical traverse mechanism mounted aboved the water surface in the wave channel. There was only negligible differences in each calibration.

The data acquisition/processing system is degined for various types of tests at Davidson Laboratory. The data acqusition program digitizes analog signals from the instruments by a analog-to-digital converter at a selected scan rate, and records them on the disk in digital form as the test progresses. After a test the spectral analysis program, which contains Fast-Fourier-Transform processing, calculates the energy density spectrum of the input signal.

3.2 Experimental parameters

All laboratory tests in the present study for the instability of the uniform wave train were conducted with various wave steepnesses between $ka=0.12$ and $ka=0.49$ by keeping the wave frequency constant at 1.1 Hz and varying wave amplitudes from 1.0 inch to 4.0 inches. Several additional tests with wave steepnesses between $ka=0.16$ and $ka=0.37$ were also performed in a different way, by keeping wave amplitude constant at 2.5 inches and varying wave frequencies from 0.8 Hz to 1.2 Hz, to investigate whether similar wave evolution and the frequency modulations are obtained at the same wave steepness but at different wave amplitude and frequency. Additional tests to obse-

rve the transverse perturbations in three-dimensional instability were also carried out and compared with that found two-dimensional instability.

4. Results

4.1 General observations

Frequently and irregularly occurring two-dimensional and three-dimensional breaking waves were observed in the evolution of the nonlinear wave train, and the initial wave steepness was crucial in deciding the type of instability and breaking.

4.1.1 Horizontal instability along the wave channel

Breaking did not occur at small wave steepness less than ka=0.19 (wave frequency, f=1.1 Hz and wave amplitude, a=1.5 inches), but small wave amplitude modulations were observed at downstream at the end of the wave evolution. At the wave steepnesses of ka=0.19 (Fig. 1) and ka=0.25 (f=1.1 Hz and a=2.0 inches), two-dimensional Benjamin-Feir instability and breaking occurred at downstream with slowly developing wave amplitude modulations before breaking location. The breaking profile was nearly uniform cross the channel and breaking process last about 10 fundamental wavelengths with reducing breaking intensity.

As the wave steepness was increased to ka=0.31 (f=1.1 Hz and a=2.5 inches), three-dimensional wave instability and breaking began to appear in the middle of evolution. At the wave steepness, ka=0.37 (f=1.1 Hz and a=3.0 inches), fully-developed three-dimensional instability was observed from the initial stage as the result of transverse perturbations cross the wave channel, which were mainly caused by the nonlinear wave interaction and the converging of the outwardly-dissipating wave energy and inwardly-reflecting wave energy by the effect of side walls of the wave channel (Fig. 2). And then, frequent, short, and small three-dimensional top-crest breaking was developed from upstream, transferring energy to the upper and the lower frequency components. This top-crest breaking results from the superharmonic instability, which has the same or less horizontal perturbation scale as the fundamental wavelength.

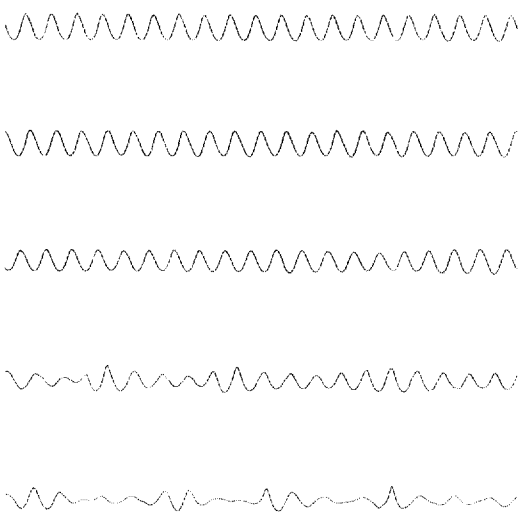

Fig. 1. Wave profiles of ka=0.19. Measuring stations at 20, 70, 120, 170, and 220 ft form the wavemaker.

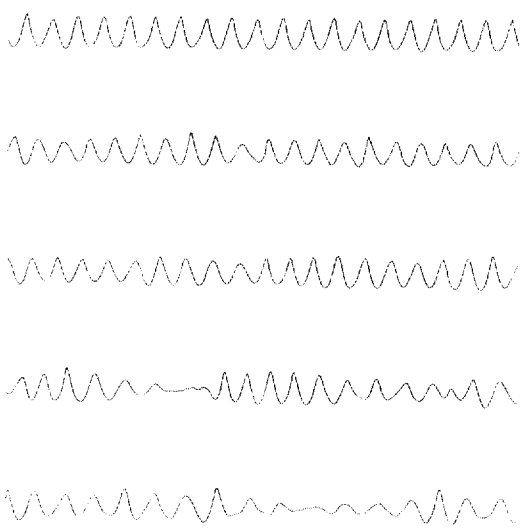

Fig. 2. Wave profiles of ka=0.37. Measuring stations at 20, 70, 120, 170, and 220 ft from the wavemaker.

As the wave train evolved to midstream, top-crest breaking transformed in its shape and became vertically asymmetric with increasing slope of the front face and deeping of the trough, so that relatively longer three-dimensional breaking due to subharmonic perturbation, which has the greater horizontal perturbation scale than the fundamental wavelength, occurred with a couple of localized breaking waves in a row. This three-dimensional instability and breaking were also observed by Melville (1982) and Su (1982) in their laboratory experiment. After that new two-dimensional second breaking occurred at downstream with weak breaking intensity. This two-dimensional second breaking, occurring in the center and at the sides of the wave channel due to slowly decaying three-dimensional instability effect, was different than the two-dimensional breaking at small wave steepness of 0.19 and 0.25, which had uniform breaking along the wave crest. After the second breaking, a series of two-dimensional wave groups was observed with significantly decreasing wave steepness.

At the wave steepness, ka=0.49 (f=1.1 Hz and a=4.0 inches), due to the initially large wave steepness, which is greater than the breaking criteria of H/L=1/7, spilling-type breaking waves occurred just after waves were generated from the wave paddle. After breaking at the wave paddle, the wave evolution was similar to that observed at the wave steepness of 0.37.

Two-dimensional and three-dimensional wave instabilities and breakings were observed at the previous tests performed by various wave steepnesses by keeping wave frequency constant and varying wave amplitude. Since the nonlinear evolution of the deep-water wave train is essentially dependent on the initial wave steepness, the similar results in the wave amplitude and frequency modulations were predicted at the same wave steepness. However, discrepancies appeared in the wave evolution, which are produced by keeping wave amplitude constant and varying wave frequency.

No breaking occurred through the wave channel in the tests of the relatively longer wave train at the wave steepnesses, ka=0.16 (f=0.8 Hz and a=2.5 inches) and ka=0.21 (f=0.9 Hz and a=2.5 inches), although second one had larger wave steepness than ka=0.19 (f=1.1 Hz and a=1.5 inches). At slightly larger wave steepness, ka=0.26 (f=1.0 Hz and a=2.5 inches), two-dimensional instability and breaking were developed in the middle of evolution. At the wave steepness, ka=0.37 (f=1.2 Hz and a=2.5 inches), the wave evolution was similar to that of the wave steepness of 0.37 (f=1.1 Hz and a=3.0 inches), but waves propagated more unstably. Short top-crest breaking was developed from the initial stage and transformed to three-dimensional breaking as approaching midstream. Two-dimensional second breaking was also observed at downstream.

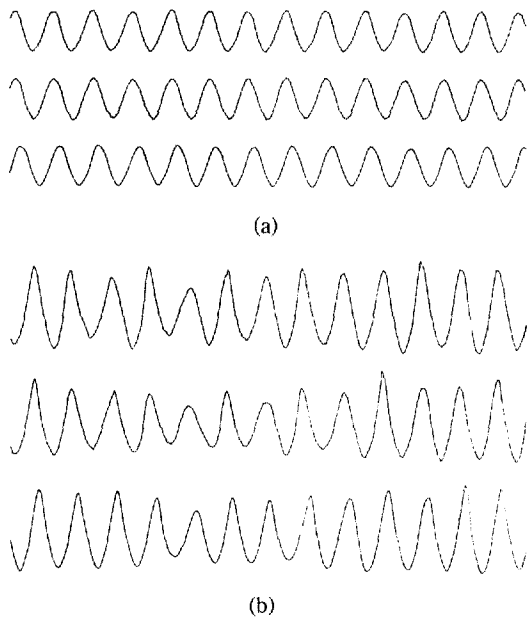

Fig. 3. Transverse wave profiles of the wave steepnesses of 0.19 (a) and 0.37 (b). Measuring stations at 1, 2, and 3 ft from one side wall.

4.1.2 Transverse instability cross the wave channel

Transverse wave profiles in two-dimensional and three-dimensional instabilities were measured at the wave steepnesses, ka=0.19 (f=1.1 Hz and a=1.5 inches) and ka=0.37 (f=1.1 Hz and a=3.0 inches). As shown in Figure 3, almost uniform transverse wave profile is observed in two-dimensional wave train, while small crestwise perturbations in wave amplitude are observed in three-dimensional instability. However, these perturbations are much smaller than those observed in the horizontal wave profile. It seems that the crestwise wave amplitude variations resulted from the effects of not only highly nonlinear wave interaction but also side walls of the wave channel, leading three-dimensional instability and finally three-dimensional breaking.

4.2 Evolution of energy density spectrum

Evolution of energy density spectrum for two-dimensional instability at the wave steepness of 0.19 (f=1.1 Hz and a=1.5 inches) is shown in Figure 4. Small magnitude of the upper and the lower side-band frequency components, apart the same value of the initial wave steepness from the fundamental wave frequency, begins to grow relatively in symmetric form in the middle of evolution around f_{upp}=1.29 Hz and f_{low}=0.91 Hz respectively. At the final stage after two-dimensional breaking, however, the lower side-band frequency is developed rapidly and becomes larger than the upper side-band frequency, showing asymmetric form. There is also shown the development of the second harmonic component from the initial stage due to small disturbances in the motion of the wave paddle. The fundamental wave frequency is dominant in the wave field through the wave evolution although its magnitude is decreased by 1/2 of the original at the final stage of the wave evolution. It is shown that at small wave steepness, the upper and the lower side-band frequencies are developed symmetrically in the non-breaking wave field, but once breaking occurs the lower side-band frequency is developed rapidly due to subharmonic perturbations and the symmetric

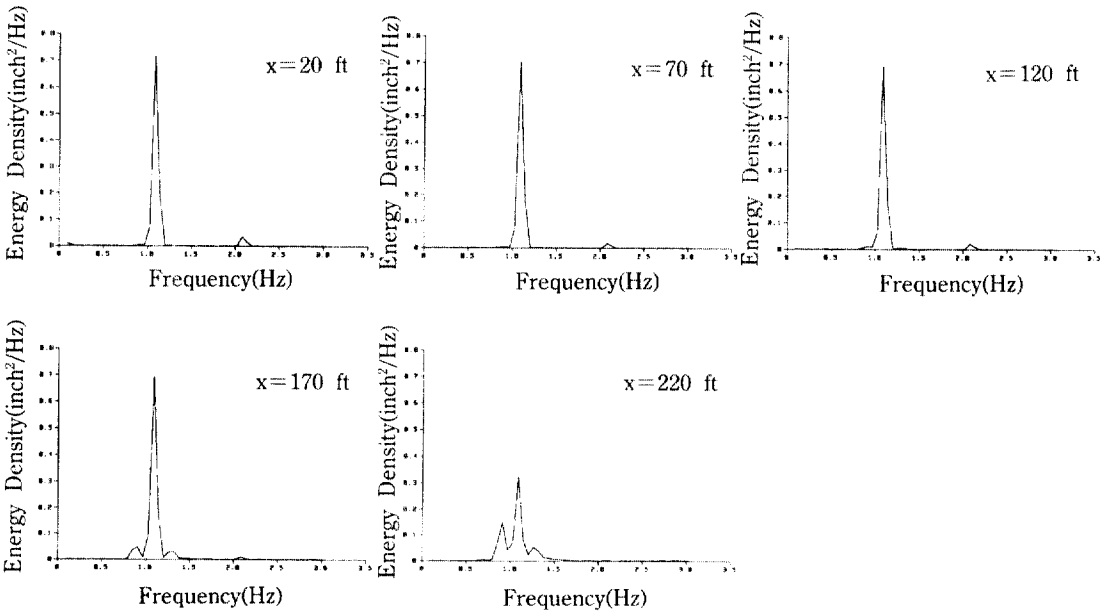

Fig. 4. Evolution of energy density spectrum at ka=0.19.

growth of the upper and the lower side-band frequencies is destroyed.

Figure 5 shows the evolution of energy density spectrum of three-dimensional instability at the wave steepness of 0.37 (f=1.1 Hz and a=3.0 inches). The fundamental wave frequency dominates in the wave field at the early stage in spite of frequent top-crest breaking with strong three-dimensional instability. It reveals that the three-dimensional top-crest breaking waves propagate primarily with the fundamental wave frequency and the superharmonic perturbation does not affect the wave frequency modulations shifting to the upper and the lower carrier wave frequencies. The magnitude of the fundamental wave frequency diminishes as the wave train propagates through the superharmonic perturbation, and the lower side-band frequency becomes dominant in the wave frequency range at the final stage after second breaking at $f_{low}=0.91$ Hz.

The occurrence of the lower side-band frequency and the frequency downshift for the uniform wave evolution are shown in Table 1. At wave steepness between 0.19 and 0.31, the upper and the lower side-band frequencies are developed at a point spaced the same value of the initial wave steepness apart from the fundamental wave frequency, but once the superharmonic perturbation is developed at large wave steepness, this consistency is destroyed and the lower side-band fre-

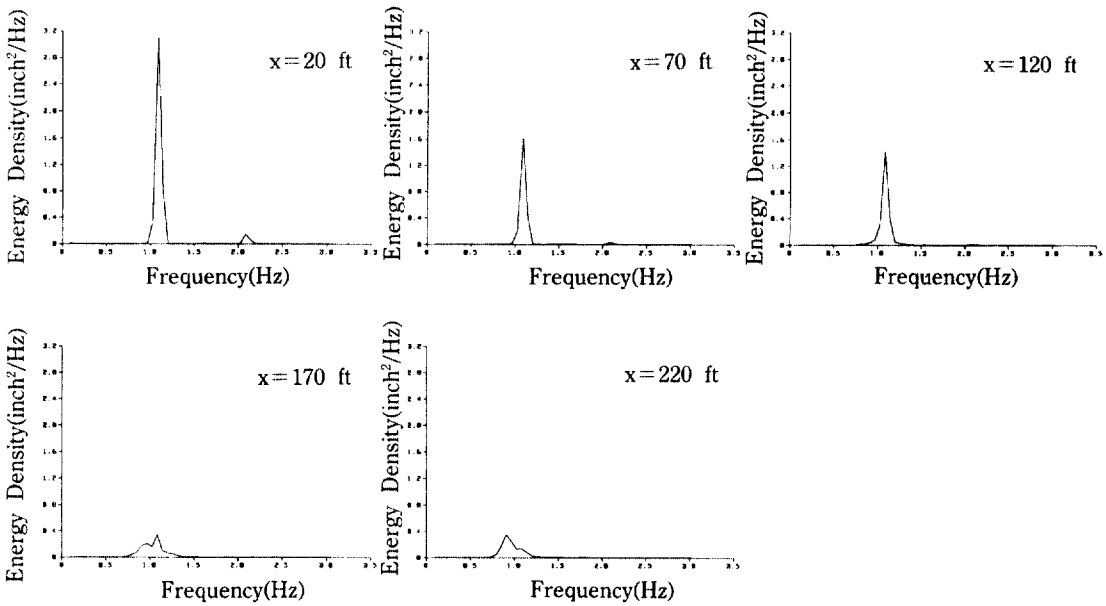

Fig. 5. Evolution of energy density spectrum at ka=0.37.

Table 1. The occurrence of the lower side-band frequency and frequency downshift

Wave steepness (ka)	Wave amplitude (a)	Wave frequency (f)	Lower side-band frequency (f_{low})	Frequency down-shift (δ)
0.19	1.5	1.1	0.91	0.19
0.25	2.0	1.1	0.85	0.25
0.31	2.5	1.1	0.79	0.31
0.37	3.0	1.1	0.91	0.19

quency grows closer to the fundamental wave frequency with smaller frequency downshift.

5. Conclusion

We have performed tests for uniform deep-water wave instability, and have watched two-dimensional and three-dimensional wave instabilities and breakings from nonlinear wave evolution.

The experimental results show that for wave steepness in the range between 0.19 and 0.25, a uniform deep-water wave train undergoes two-dimensional Benjamin-Feir instability and ultimately leads to breaking as the wave train evolves downstream. At the wave steepness of 0.31, three-dimensional instability and breaking begin to appear, and at large wave steepness greater than or equal to 0.37, top-crest breaking with fully-developed three-dimensional instabilty, showing superharmonic structure, is developed from the early stage as transverse perturbations grow rapidly cross the wave channel. This top-crest breaking is transformed to the relatively longer localized three-dimensional breaking with subharmonic structure as the wave train propagates midstream. Two-dimensional second breaking is observed at the end of evolution with significantly decreased wave steepness.

During the initial stage, the fundamental wave frequency is dominant in the wave evolution without significant growth of the side-band frequencies. As the wave train propagates, the lower side-band frequency begins to develope with wave energy spreading to many frequency components. At large wave steepness, the lower side-band frequency grows rapidly and becomes the dominant carrier frequency after second breaking at the final stage. At small wave steepness, the major lower sied-band frequency is developed at a point on the frequency range, apart the same value of the initial wave steepness from the fundamental wave frequency. However, once superharmonic perturbation with top-crest breaking arise at the early stage at large wave steepness, the major lower side-band frequency is developed near the fundamental wave frequency with smaller frequency downshift.

The similar results of wave evolution and frequency modulations are expected at the nearly same initial wave steepness, either varying wave amplitude with constant wave frequency or varying wave frequency with constant wave amplitude. However, discrepancies exhibits in both wave evolution and frequency modulations due to difference in propagating wave energy. The shorter waves with smaller wave amplitude are modulated more severely from the initial stage with faster growing lower side-band frequency, and breaking is developed earlier than the longer waves with large wave amplitude. It can be inferred that the evolution of a nonlinear deep-water wave train is dependent not only on the initial wave steepness but also on wave amplitude and frequency.

References

1. 1. Benjamin, T. B. and Feir, J. E. 1967, "The disintegration of wave trains in deep water, Part 1. Theory", *J. Fluid Mech.* 27, 417-430.
2. Crawford, D. R., Lake, B. M., Saffman, P. G. and Yeun, H. C. 1981, "Stability of weakly nonlinear deep-water waves in two and three-dimensions", *J. Fluid Mech.* 105, 177-191.
3. Crawford, D. R., Lake, B. M., Saffman, P. G. and Yeun, H. C. 1981, "Effects of nonlinearity and spectral bandwidth on the dispersion relation and component phase speeds of surface gravity waves", *J. Fluid Mech.* 112, 1-32.
4. Lake, B. M., Yeun, H. C., Rungaldier, H. and Ferguson, W. E. 1977, "Nonlinear deep-water waves: theory and experiment. Part 2. Evolution of a continuous wave tarin", *J. Fluid Mech.* 83, 49-74.
5. Lake, B. M. and Yeun, H. C. 1977, "A note on some nonlinear water-wave experiments and the comparison of data with theory", *J. Fluid Mech.* 83, 75-81.
6. Longuet-Higgins, M. S. 1978a, "The instability of

gravity waves of infinite amplitude in deep water. I. Superharmonics", *Proc. R. Soc.* Lond. A 360, 471-488.
7. Longuet-Higgins, M. S. 1978b, "The instability of gravity waves of infinite amplitude in deep water. II. Subharmonics", *Proc. R. Soc.* Lond. A360, 489-505.
8. McLean, J. W. 1982, "Instabilities of finite-amplitude water waves", *J. Fluid Mech.* 114, 315-330.
9. Melville, W. K. 1982, "The instability and breaking of deep-water waves", *J. Fluid Mech.* 115, 165-185.
10. Melville, W. K. 1983, "Wave modulation and breakdown", *J. Fluid Mech.* 128, 489-506.
11. Melville, W. K. and Rapp, R. J. 1988, "The surface velocity field in steep and breaking waves", *J. Fluid Mech.* 189, 1-22.
12. Su, M., Bergin, M., Marler, P. and Myrick, R. 1982, "Experiments on nonlinear instabilities and evolution of steep gravity-wave train", *J. Fluid Mech.* 124, 46-72.

(接受 : 1993. 1. 25)